Atmospheric Environment 333 (2024) 120653

Contents lists available at ScienceDirect

Atmospheric Environment

journal homepage: www.elsevier.com/locate/atmosenv

Mesoscale wind field patterns conducive to the high-$PM_{2.5}$ episodes over South Korea: Cluster analysis

Daniel Choi [a,b], Jeeyoung Ham [a,c], Gookyoung Heo [a,d], Soon-Hwan Lee [e], Jung-Woo Yoo [f], Geum-Hee Yang [g,h], Sohyun Jeon [i,j], Cheol-Hee Kim [f,h,*]

[a] National Air Emission Inventory and Research Center, Ministry of Environment, Cheongju, South Korea
[b] Now at The Robert H. Smith Faculty of Agriculture, Food and Environment, Department of Soil and Water Sciences, The Hebrew University of Jerusalem, Rehovot, Israel
[c] Department of Earth and Environmental Sciences, Korea University, Seoul, South Korea
[d] Now at Environmental Satellite Center, National Institute of Environmental Research, Incheon, South Korea
[e] Department of Earth Science Education, Pusan National University, Busan, South Korea
[f] Institute of Environmental Studies, Pusan National University, Busan, South Korea
[g] Climate and Air Quality Research Department, National Institute of Environmental Research, Incheon, South Korea
[h] Department of Atmospheric Sciences, Pusan National University, Busan, South Korea
[i] Environmental Health Research Department, National Institute of Environmental Research, Incheon, South Korea
[j] Department of Environmental Engineering, Konkuk University, Seoul, South Korea

HIGHLIGHTS

- Mesoscale wind patterns for high $PM_{2.5}$ episodes in South Korea are presented.
- Mesoscale wind patterns well compared between local and transported patterns.
- Dominant wind patterns correlated with geographical locations in Korea.
- Patterns can be a reference for aircraft-based campaign studies over Korea.

ARTICLE INFO

Keywords:
Mesoscale wind field pattern
High $PM_{2.5}$ episodes
K-means clustering
Mitigation strategy in South Korea

ABSTRACT

Mesoscale wind field patterns play important roles in episodes of high particulate matter ($PM_{2.5}$). Previous studies have reported the main synoptic meteorological features associated with high-$PM_{2.5}$ days with two primary modes: long-range transport (LRT) and stagnation or local contribution (STL). However, due to the lack of more small-scale analyses spanning across multiple administrative regions, statistical quantification of representative mesoscale wind patterns with elevated $PM_{2.5}$ episodes is needed to explore region-specific emissions reduction strategies in South Korea. This study applied *k*-means clustering to NCEP FNL reanalysis data from 2016 to 2020 to identify mesoscale wind field patterns associated with high-$PM_{2.5}$ episodes across all 17 administrative regions of South Korea. Our statistical approach yielded region-specific wind fields for 17 individual administrative regions, and also empirically yielded a total of eight representative patterns, four patterns each for both LRT and STL modes, which were applicable across all regions. The eight patterns were consistent with most previous studies. In addition, we quantified the LTP and STL modes in all 17 regions, and showed that they were more prevalent in the western and southeastern administrative regions of South Korea, respectively. Our results serve as a reference for region-specific mitigation strategies in all administrative regions of South Korea, and will also be useful for analyzing relations between meteorology and high-$PM_{2.5}$ episodes in the SIJAQ and ASIA-AQ studies.

* Corresponding author. Department of Atmospheric Sciences, Pusan National University, 2 Busandaehak-ro 63beon-gil, Geumjeong-gu, Busan, 46241, South Korea.
E-mail address: chkim2@pusan.ac.kr (C.-H. Kim).

https://doi.org/10.1016/j.atmosenv.2024.120653
Received 2 April 2024; Received in revised form 27 May 2024; Accepted 11 June 2024
Available online 12 June 2024

1. Introduction

Particulate matter (PM), particularly ultrafine particles ($PM_{2.5}$ with diameter <2.5 μm), has significant adverse effects on both air quality and public health. Elevated levels of $PM_{2.5}$ pollutants in South Korea have prompted the enhancement of governmental policies for PM mitigation and the implementation of stricter measures for reducing emissions (Kim et al., 2018a; Park et al., 2020). In Korea, the levels of $PM_{2.5}$ and other air pollutants are influenced by middle- or synoptic-scale weather patterns and the local emission of pollutants (Ham et al., 2021; Lee et al., 2019a; Seo et al., 2017). There have been many studies of the causes of high-$PM_{2.5}$ episodes in Korea. Such episodes have occurred frequently in urban areas since the mid-2010s due to both transboundary, transported $PM_{2.5}$ and locally emitted pollutants (Kim et al., 2012, 2021a; Lee et al., 2014).

Such episodes occur intricately depending on mesoscale meteorological conditions, and impact assessments of meteorological conditions on $PM_{2.5}$ are still quite challenging. For example, higher temperatures favor sulfate formation while low temperatures favor nitrate formation. The relations between urban $PM_{2.5}$ pollution and synoptic-scale circulation have been verified in a number of previous studies (Lee et al., 2013; Oh et al., 2015, 2020; Seo et al., 2017, 2018; Wang et al., 2018; Zhao et al., 2018). The weakening of the so-called Siberian High in January 2013 reduced the northwesterly winds, causing severe PM pollution events over China (Zhao et al., 2018), and a stationary blocking high pressure zone was identified as the reason for severe haze episodes in Korea (Chang et al., 2021; Seo et al., 2017). In addition, a stationary or slow-moving anticyclone located over southwestern China was shown to generate westerly or northwesterly winds that are conducive to transboundary high-$PM_{2.5}$ episodes over Korea. As specific synoptic or micro-meteorological conditions are strongly associated with high-$PM_{2.5}$ episodes (Kim et al., 2023; Oh et al., 2024), quantitative approaches involving analysis of mesoscale meteorology and regional PM are needed to be able to devise quantitative mitigation strategies in administrative regions. However, few studies have addressed this topic to date.

Research on meteorological influences on air quality often use statistical methods, such as cluster analysis, to identify wind field patterns affecting high PM concentrations (Jeon et al., 2019; Kim et al., 2006; Lee et al., 2011). Principal component analysis (PCA), regression analysis, and *k*-means or multivariate clustering have been used in many previous studies (Choi et al., 2023; Jeon et al., 2019; Kim et al., 2017; Kim et al., 2018b; Leung et al., 2018; Tai et al., 2012). However, such studies have predominantly focused on specific cities or events with extremely high pollution levels, and there have been few comprehensive studies on a nationwide scale encompassing all administrative regions in South Korea.

The present study was performed using data collected between 2016 and 2020 to analyze the prevailing wind field patterns associated with high-$PM_{2.5}$ episodes across all 17 administrative regions of South Korea. We first identified mesoscale wind field patterns on high-$PM_{2.5}$ days by simple *k*-means clustering of data from the National Center for Environmental Prediction (NCEP) and National Center for Atmospheric Research (NCAR), and characterized the contributions of each pattern to region-specific $PM_{2.5}$ episodes in each administrative region. Determination of the meteorological conditions driving high-$PM_{2.5}$ episodes in the 17 administrative regions would provide insights that could help facilitate the development of tailored region-specific mitigation strategies.

In addition, we attempted to determine representative wind field patterns applicable across all regions in South Korea. Our method provided insight into several representative wind field features influencing high-$PM_{2.5}$ levels across the administrative regions of South Korea, and the results improve understanding of the impacts of wind fields on $PM_{2.5}$ pollution. Furthermore, our findings will be useful for diagnosing meteorological factors contributing to high-$PM_{2.5}$ episodes in aircraft-based projects over South Korea and Asian regions, such as the Satellite Integrated Joint Monitoring of Air Quality (SIJAQ) and Airborne and Satellite Investigation of Asian Air Quality (ASIA-AQ) studies launched in 2021–2022 or planned to launch in 2024.

2. Methods and data used

2.1. Study area

This study included all 17 administrative regions of South Korea consisting of the capital city, Seoul (SL), six metropolitan cities (Busan (BS), Daegu (DG), Incheon (IC), Gwangju (GJ), Daejeon (DJ), and Ulsan (US)), six provinces (Gyeonggi-do (GG), Chungcheongbuk-do (CB), Chungcheongnam-do (CN), Jeollanam-do (JN), Gyeongsangbuk-do (GB), and Gyeongsangnam-do (GN)), three special self-governing provinces (Gangwon-do (GW), Jeonbuk-do (JB), and Jeju-do (JJ)), and one special self-governing city (Sejong (SJ)) (Fig. 1).

Most previous studies have focused on the Seoul Metropolitan Area (SMA), a highly urbanized area consisting of Seoul, Incheon, and Gyeonggi-do with a population of 26.1 million, which experiences significant levels of $PM_{2.5}$ due to both local emissions and the transboundary transport of air pollutants (Jo and Kim, 2013; Kim et al., 2012; Park et al., 2005, 2021). The annual PM with diameter <10 μm (PM_{10}), nitric oxide and nitrogen dioxide (NOx), and volatile organic compounds (VOCs) emissions in 2015 in SMA were 50,603 tons, 297,833 tons, and 305,928 tons, respectively, and PM_{10} and NOx emissions were mainly from traffic (NIER, 2018). By contrast, the cluster of Busan, Ulsan, and Gyeongsangnam-do, located in southeastern South Korea, consists of a mix of urban and port areas with a total population of 7.6 million, where PM sources can vary from vehicles to shipping activities (Kim et al., 2021b). In Busan, annual PM_{10}, NOx, and VOCs emissions in 2015 were approximately 27,303 tons, 185,572 tons, and 242,220 tons, respectively, corresponding to approximately half of those in Seoul. High traffic density was considered to be responsible for a large proportion of these emissions in this region (Yang et al., 2020). The differences in emissions characteristics, local meteorological features, and geographic locations between administrative regions indicate the need for region-specific strategies to manage and mitigate high-$PM_{2.5}$ episodes in South Korea.

2.2. Cluster analysis

To categorize the representative mesoscale wind field patterns that contribute to high-$PM_{2.5}$ episodes, *k*-means cluster analysis was performed using reanalysis meteorological data and surface $PM_{2.5}$ measurements across all administrative regions in South Korea (Fig. 1). We applied the *k*-means method, a well-established technique for nonhierarchical clustering based on data proximity, as documented previously (Carro-Calvo et al., 2017; Darby, 2005; Jeon et al., 2019; Souri et al., 2016).

To determine the optimal number of clusters (k) for accurate classification, we calculated the within-group sum of squares (WSS) between cluster centroids ($\overline{x}_k$) and corresponding data ($\overline{x}_{ik}$)(Jin et al., 2011), which diminishes as k increases and stabilizes at a threshold, indicating the most representative value of k for the analysis as follows:

$$WSS = \sum_{1}(x_{i1}-\overline{x}_1)^2 + \sum_{2}(x_{i2}-\overline{x}_2)^2 + \ldots + \sum_{k}(x_{ik}-\overline{x}_k)^2$$

Upon establishing the optimal k, we assigned each data point to the nearest cluster centroid, iterating the process 1000 times to ensure robust cluster determination. Prior to *k*-mean clustering, determination of cluster number was required in each of the administrative regions. We estimated the optimal number of clusters based on diagnosis of the divergence of WSS values by gradually increasing the number of clusters in each administrative region (Fig. S1), instead of starting the K-means cluster analysis with a predetermined number of clusters. We employed

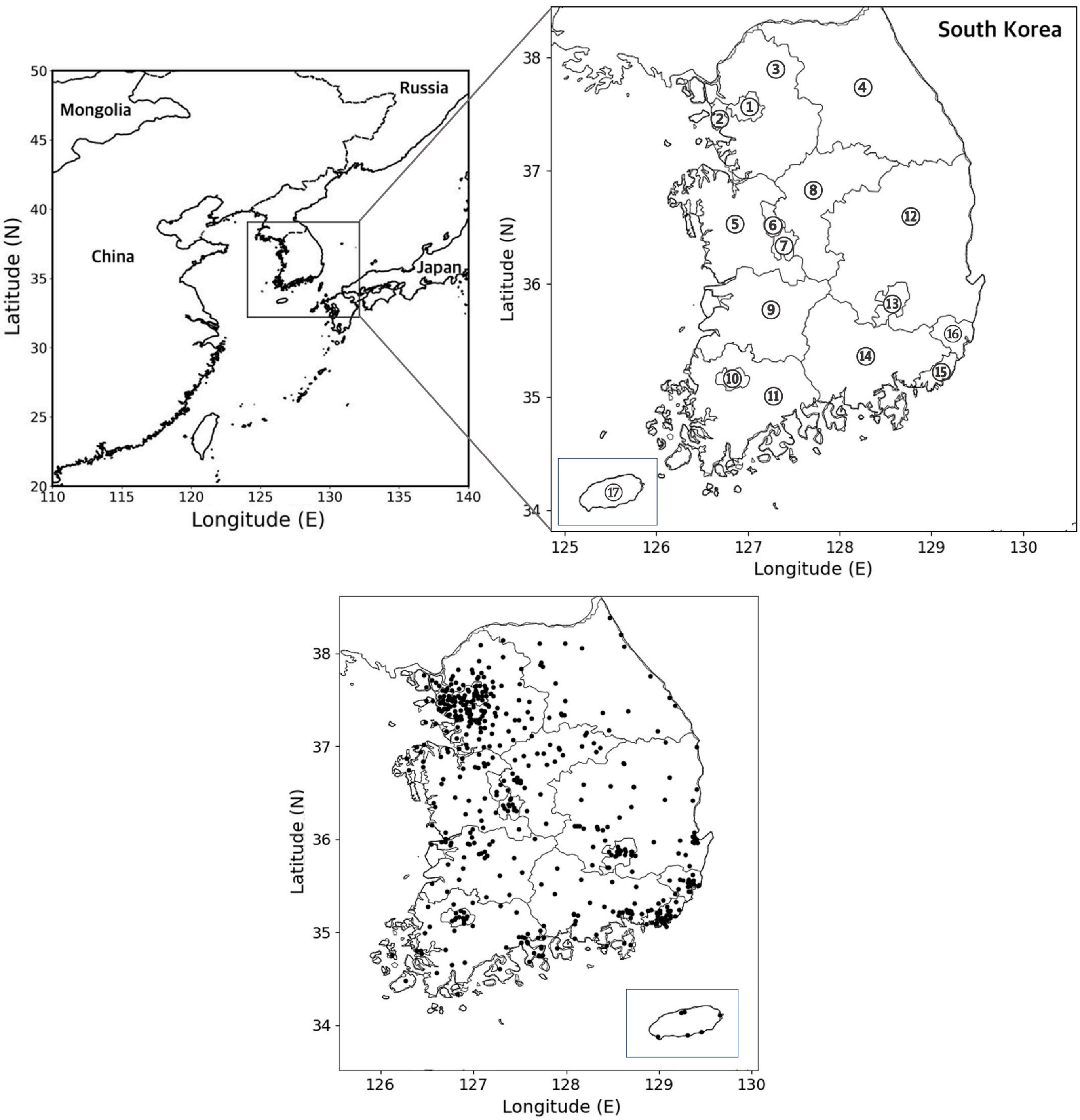

Fig. 1. (Top) Study area and locations of the 17 administrative regions of South Korea: ① Seoul (SL), ② Incheon (IC), ③ Gyeonggi-do (GG), ④ Gangwon-do (GW), ⑤ Chungcheongnam-do (CN), ⑥ Sejong (SJ), ⑦ Daejeon (DJ), ⑧ Chungcheongbuk-do (CB), ⑨ Jeonbuk-do (JB), ⑩ Gwangju (GJ), ⑪ Jeollanam-do (JN), ⑫ Gyeongsangbuk-do (GB), ⑬ Daegu (DG), ⑭ Gyeongsangnam-do (GN), ⑮ Busan (BS), ⑯ Ulsan (US), and ⑰ Jeju-do (JJ). (Bottom) Locations of air quality monitoring stations (AQMS) over the 17 administrative regions in South Korea.

an iterative technique, starting with fewer clusters and incrementally increasing. This methodology enabled a statistically reliable identification of the optimal cluster count, ensuring meaningful data representation in each cluster while preventing overfitting. Further information can be found in previous reports (Carro-Calvo et al., 2017; Jeon et al., 2019).

Upon identifying clusters within each of the 17 administrative regions, we conducted empirical merging to consolidate similar clusters, ensuring that the grouping was based on their associated wind field patterns for each of the four seasons and their relevance to $PM_{2.5}$ pollution. This iterative refinement aimed to enhance the representation of typical wind patterns within the clusters. Subsequently, we classified them into distinct major groups, including LRT and STL modes, following the criteria proposed by Jo and Kim (2013). It is important to note that while patterns may match each other, biases between patterns are expected due to the inherent variability of atmospheric conditions, but we do not expect the biases to change the key findings of the present study.

2.3. $PM_{2.5}$ and meteorological data

We used hourly surface observational air quality data from the air quality monitoring stations (AQMS) managed by the Korean Ministry of Environment and local governments in South Korea. The observed $PM_{2.5}$ data were averaged in all of 17 administrative regions and used in the analysis. The AQMS network (Fig. 1) records real-time pollutant levels, providing hourly data for CO, NO_2, SO_2, O_3, as well as $PM_{2.5}$ and PM_{10}. For our purposes, we compiled data of high-$PM_{2.5}$ pollution days spanning from 2016 to 2020, after the initiation of $PM_{2.5}$ monitoring in mid-2015, and selected high-$PM_{2.5}$ days during the study period (from 2016 to 2020) and characterized the number of high-$PM_{2.5}$ days and also associated those with wind fields across the administrative regions.

The high-$PM_{2.5}$ days were categorized as those with daily average $PM_{2.5}$ levels $\geq$35 μg/m^3, which were classified as having "poor" or "very poor" air quality according to the 4-rating South Korean air quality index: "good," "moderate," "poor," and "very poor." $PM_{2.5}$ data are available from the Air Korea website (https://www.airkorea.or.kr/) operated by the Korea Environment Corporation. Cases involving yellow dust were excluded. Locations of AQMS that monitor the $PM_{2.5}$ concentrations are also indicated in Fig. 1.

With regard to the wind field data, we utilized 5 years of gridded meteorological data covering East Asia, including pressure fields and wind speed/direction data at 900 hPa from the FNL Operational Global Analysis with a resolution of 1° × 1°, provided by NCEP/NCAR. The NCEP/NCAR FNL data are available in the NCAR Research Data Archive (RDA) (https://rda.ucar.edu).

3. Results and discussion

3.1. Regional features of high-$PM_{2.5}$ events

Table 1 list the numbers of days with "poor" or "very poor" air quality of $PM_{2.5}$ by season during 2016–2020, and Fig. 2 shows the regional distributions of cumulative numbers of days. The data indicate distinct seasonal variation in number of days across the regions, again indicating the importance of pollution emissions and meteorology. With regard to seasonal characteristics according to each region, in spring, the JB region had the highest occurrence of high-$PM_{2.5}$ days at 134, followed by GG with 124 days. By contrast, GN, geographically situated further to the south, had fewer high-$PM_{2.5}$ days with a total of 47 days. There were generally fewer high-$PM_{2.5}$ days nationwide in summer, with DJ having the fewest (only 5 days). Notable exceptions were observed in regions such as US with the highest at 59 days and BS at 43 days. These two regions are located to the southeast of South Korea, where the influence of secondary formation of sulfates from port emissions during the summer is assumed to be significant (Kim et al., 2021b; Yang et al., 2020). These results underscore the factors to be considered in estimating seasonal and regional disparities between regions. Two regions, i.e., US and BS, with high proportions of high-$PM_{2.5}$ days during summer (Fig. 2), indicated a special need for season-specific policies to reduce $PM_{2.5}$ levels in these areas.

Marked increases in high-$PM_{2.5}$ days were seen in fall, particularly in JB where 87 days were recorded, indicating susceptibility to PM between summer and winter. However, high-$PM_{2.5}$ days peaked during winter across the administrative regions, with CB experiencing the most at 194 days. Over the 5-year span, CB had the greatest number of $PM_{2.5}$ days at 415, while JJ had the fewest at 136, underscoring continuous marine impacts in the JJ region even in winter.

3.2. Results of cluster analysis

3.2.1. K-mean clustered wind patterns affecting high $PM_{2.5}$

Fig. S1 illustrates WSS against the number of clusters in the *k*-means clustering algorithm for all 17 administrative regions. The results show that the majority of the regions stabilized at 3–5 clusters, suggesting that

Table 1
Number of high-$PM_{2.5}$ days by season in 17 administrative regions of South Korea in 2016–2020.

Season	SL	BS	DG	IC	GJ	DJ	US	SJ	GG	GW	CB	CN	JB	JN	GB	GN	JJ	Total
Spring	113 (37%)	84 (34%)	53 (22%)	103 (38%)	76 (30%)	53 (30%)	**91 (36%)**	67 (28%)	124 (34%)	102 (39%)	122 (29%)	96 (32%)	134 (33%)	55 (40%)	76 (30%)	47 (31%)	**55 (40%)**	1451
Summer	28 (9%)	43 (17%)	14 (6%)	21 (8%)	13 (5%)	5 (3%)	59 (23%)	12 (5%)	21 (6%)	12 (5%)	16 (4%)	13 (4%)	33 (8%)	7 (5%)	10 (4%)	21 (14%)	9 (7%)	337
Autumn	40 (13%)	34 (14%)	55 (23%)	42 (16%)	55 (22%)	27 (15%)	34 (13%)	38 (16%)	61 (17%)	28 (11%)	83 (20%)	56 (19%)	87 (22%)	15 (11%)	52 (21%)	22 (14%)	17 (13%)	746
Winter	**127 (41%)**	**86 (35%)**	**122 (50%)**	**104 (39%)**	**108 (43%)**	**94 (53%)**	68 (27%)	**123 (51%)**	**163 (44%)**	**122 (46%)**	**194 (47%)**	**131 (44%)**	**150 (37%)**	**60 (44%)**	**115 (45%)**	**62 (41%)**	**55 (40%)**	**1884**
Total	308	247	244	270	252	179	252	240	369	264	415	296	404	137	253	152	136	4418

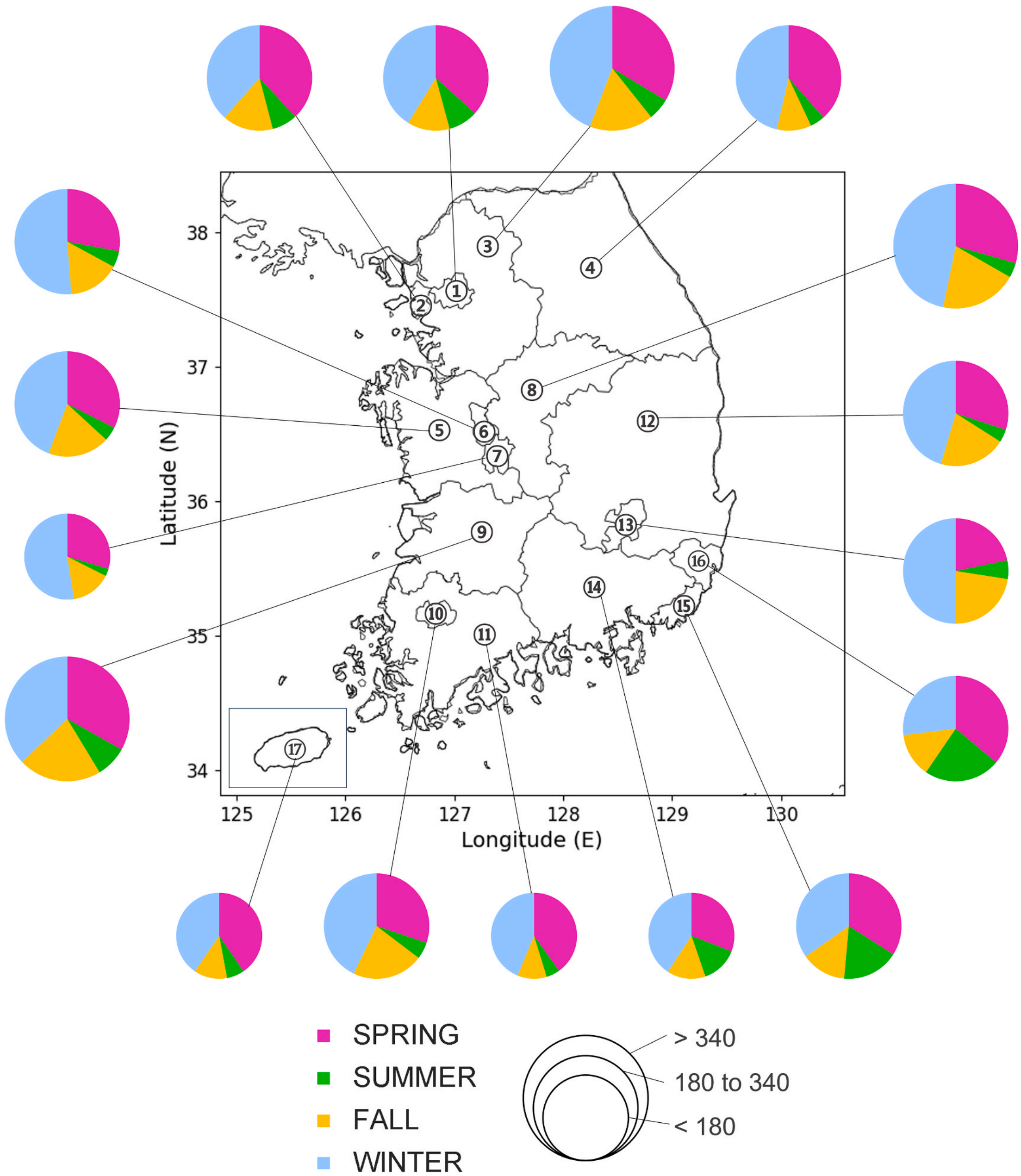

Fig. 2. Pie charts showing seasonal cumulative numbers of days with "poor" or "very poor" air quality with regard to $PM_{2.5}$ in each administrative region in South Korea from 2016 to 2020. The number representing each of the 17 administrative regions is indicated in Fig. 1.

the number of representatives would be relatively small. Incheon (IC) only aligned with five clusters, reflecting more intricate meteorological interactions possibly due to the combination of both coastal and urban characteristics. By choosing the appropriate number of clusters (Fig. S1), we extracted 3–5 representative wind field patterns for each administrative region.

The extracted 900 hPa mesoscale wind field patterns for the selected number of clusters were named according to the region + cluster number e.g., SL_C1 for the first representative cluster of wind field in Seoul (SL). We hypothesized that the 900 hPa level wind fields would effectively represent both the friction-free upper atmosphere and the lower atmosphere influenced by friction. Fig. 3 illustrates the horizontal representative wind field patterns for Seoul, and Table 2 shows the occurrence frequencies of each representative wind field pattern.

The first cluster, SL_C1, was the most prevalent pattern with a frequency of 29.5%, and was characterized by weak northwesterly winds over the Korean Peninsula during both winter and early spring (Table 2). This pattern was characterized by a zone of high pressure in central China (Fig. 3), and therefore facilitated the transport of pollutants from northeastern China or North Korea. Cluster SL_C2, with a frequency of 21.8%, was characterized by southwesterly winds caused by migrating anticyclones centered over the western islands of Japan. This pattern was prevalent during spring and winter. Cluster SL_C3, with a frequency of 20.8%, consisted of days with dominant northwesterly winds in winter (Table 2), influenced by emissions from northeastern China. Finally, SL_C4, with a frequency of 27.9%, was marked by weak synoptic winds produced by anticyclones located directly above the Korean Peninsula, particularly in spring and early summer, conducive to the accumulation of local pollution.

All representative wind field patterns for the remaining 16 administrative regions are illustrated in Fig. S2. Some of the administrative regions were characterized by inflow of wind field patterns similar to

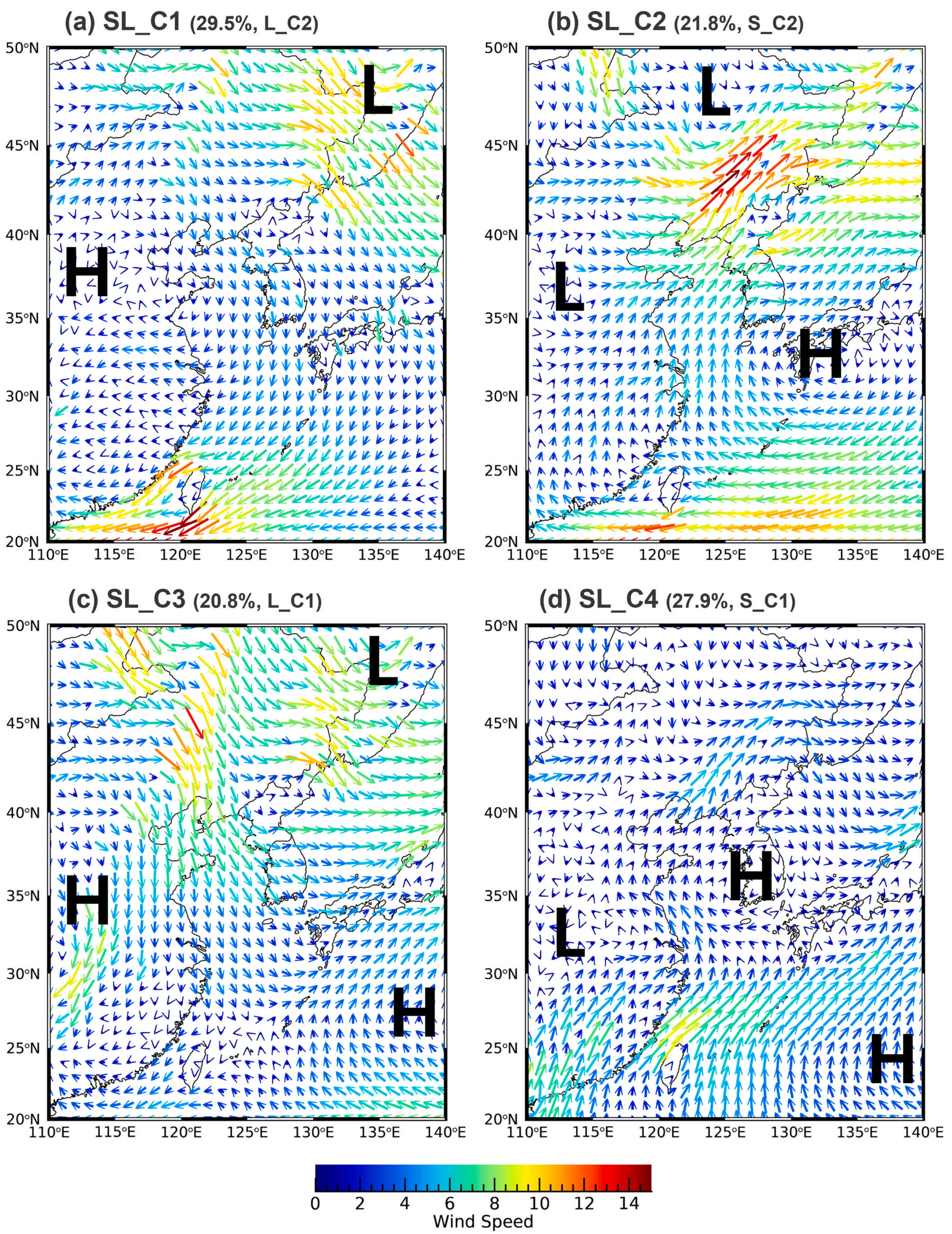

Fig. 3. Horizontal distributions of representative wind field patterns associated with high-$PM_{2.5}$ episodes in Seoul (SL) (2016–2020): cluster 1–4, identified by *k*-means clustering, with percentages indicating the contribution of each pattern to high-$PM_{2.5}$ episodes.

Table 2
Average $PM_{2.5}$ concentrations and occurrence frequencies of four representative mesoscale wind field patterns by season in Seoul (SL) in 2016–2020.

Cluster	$PM_{2.5}$ (μg/m^3)	Spring	Summer	Fall	Winter	Total
SL_C1	48.8	23	0	18	50	91
SL_C2	50.2	23	2	11	31	67
SL_C3	48.9	18	0	7	39	64
SL_C4	45.1	49	26	4	7	86
Total	48.1	113	28	40	127	308

Table 3
Number of occurrences by representative mesoscale wind field clusters across the 17 administrative regions.

Cluster	Distinct Wind Field	Counts
S_C1	STL Weak Synoptic Stagnation	9
S_C2	STL Southwesterly	5
S_C3	STL Weak Southwesterly	12
S_C4	STL Weak Southerly	1
L_C1	LRT Northwesterly	15
L_C2	LRT Weak Northwesterly	11
L_C3	LRT Westerly	2
L_C4	LRT Northerly	2

those seen in areas with anticyclones. For example, anticyclones located to the west of the Korean Peninsula or inland Near East China mostly induced weak winds over the Korean Peninsula. Most high-pressure areas around the direct Korean Peninsula were related to accumulation of $PM_{2.5}$ within the Korean Peninsula (Fig. S2).

We attempted to empirically merge such similar patterns, and identified a total of eight representative wind fields applicable across all regions of the Korean Peninsula (Fig. 4). Finally, we distinguished eight patterns that were prevalent over the Korean Peninsula in two distinct modes, i.e., long-range transport (LRT) and stagnation or local contribution (STL) modes, based on the wind flow: inflow, outflow, and stagnant/transboundary patterns. The classified eight patterns were verified by employing the criteria for distinguishing LRT and STL (Jo and Kim, 2013), ultimately divided into four for LRT mode and four for STL mode.

Table 3 shows the reclassified two representative modes, LRT and STL, and Fig. 4 shows each of the eight representative wind field patterns (four patterns for each of LRT and STL modes). The first pattern belonged to STL mode and was mostly characterized by eastward migrating anticyclones (Fig. 4). Migratory anticyclones passing close to the Korean Peninsula induced a weak synoptic field (S_C1), which enhanced stagnation near the center of the anticyclone over the Korean Peninsula, exacerbating the accumulation of pollutants in South Korea (Jo and Kim, 2013). If an anticyclone over South Korea shifts further eastward, it can prompt southwesterly (S_C2), weak southwesterly (S_C3), and weak southerly winds (S_C4). While these three southerly and weak wind field patterns typically transport clean air to downstream areas, they can also at times cause local recirculation of pollutants through land–sea breezes due to the low wind speed (Hwang et al., 2007; Oh et al., 2006), preventing $PM_{2.5}$ moving toward outer regions (Fig. 4 and Table 3).

On the other hand, the LRT mode is governed by northwesterly wind series (westerly, northwesterly, and northerly) (Table 3) due to the presence of continental anticyclones, which are favorable for transboundary migration of $PM_{2.5}$ pollutants and precursors into the Korean

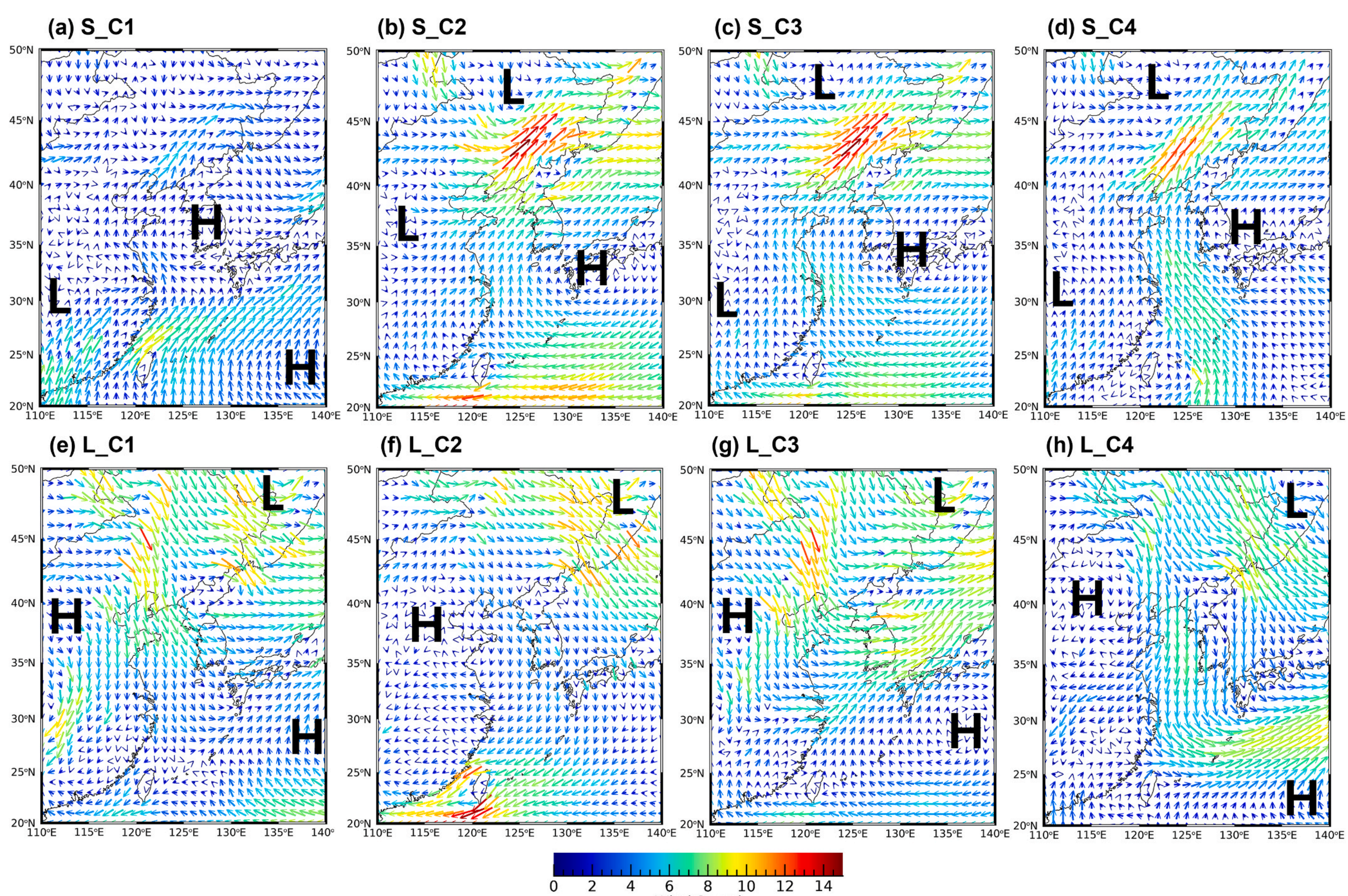

Fig. 4. Eight representative wind field patterns associated with high-$PM_{2.5}$ episodes in South Korea. (a) Weak synoptic stagnation (S_C1). (b) Southwesterly (S_C2). (c) Weak Southwesterly (S_C3). (d) Weak Southerly (S_C4). (e) Northwesterly (L_C1). (f) Weak Northwesterly (L_C2). (g) Westerly (L_C3). (h) Northerly (L_C4).

Peninsula, as discussed previously (Choi et al., 2023; Jeon et al., 2019; Lee et al., 2019b). It is also notable that this LRT wind field pattern was more prevalent in winter when the Siberian anticyclone is developing and extending to the Korean Peninsula. We ultimately separated these into four distinct wind field patterns: northwesterly (L_C1), weak Northwesterly (L_C2), westerly (L_C3), and northerly (L_C4) (Fig. 4 and Table 3).

The eight representative patterns identified in this study are fairly consistent with previous studies. Chang et al. (2021) performed a similar study on high-$PM_{2.5}$ episodes over SMA from 2016 to 2018 using PCA. Although their study area was not nationwide but limited to the SMA, they reported several wind field patterns for high-$PM_{2.5}$ episodes. For example, when onshore anticyclones moved into the Korean Peninsula, the northwest flows prevailed with LRT mode, resembling the wind patterns in Fig. 4(e) and (f) of the present study. Conversely, typical wind patterns when offshore high-pressure systems exited from the Korean Peninsula to the east or northeast contributed to high $PM_{2.5}$ concentrations in STL mode over the SMA, consistent with our patterns shown in Fig. 4(b)–(d). Jeon et al. (2019) applied the *k*-means clustering technique in association with PM_{10} episodes and classified wind patterns from 2012 to 2016 over the SMA. For high-PM_{10} days, they classified five wind patterns denoted as C_H1 to C_H5. Comparing our results with these patterns, C_H1 and C_H3 corresponded fairly well with the patterns shown in Fig. 4(a) and (c), respectively. Despite the slight discrepancies, C_H4 was similar to the patterns in Fig. 4(e) and (g). However, our results did not include a pattern similar to C–H2 because they defined C_H2 as yellow dust events, while these were not included in the present study.

3.2.2. Wind field patterns by administrative region

We further attempted to delineate the region-specific representative mesoscale wind field patterns in a quantitative manner in each of the 17 administrative regions. By matching the region-by-region patterns shown in Fig. S2 to the clustered STL and LRT modes, we could quantitatively determine which mode was dominant in all administrative regions. Table 4 and Table S1 show the estimated region-specific statistics of dominance between the two modes. The results showed that the northwesterly L_C1 pattern was dominant in 15 regions, which makes it the most widespread pattern across South Korea. The prevalence of the LRT mode emphasized the distinct role of transboundary transport in the occurrence of high-$PM_{2.5}$ episodes (see Table 4, Table S1, and Fig. S2). Notably, the L_C1 and L_C2 clusters were both predominant in some regions, such as JB and JJ, indicating the influence of long-distance transport of pollution toward these areas.

By contrast, closer examination of Table S1 also illustrates the complexity of mechanisms of high-$PM_{2.5}$ episodes, i.e., transitioning from STL to LRT, or vice versa. For example, in the BS region, a significant majority of high-$PM_{2.5}$ days were associated with the STL mode particularly under the S_C1 pattern, underscoring the influence of local conditions on high $PM_{2.5}$ favorable for the accumulation of pollutants. This highlighted the complexity of differences between regions reflecting local characteristics.

Fig. 5 shows the distributions of STL and LRT contributions to the high-$PM_{2.5}$ episodes in each of the 17 administrative regions. SL showed equal contributions of the two modes. While the LRT mode tended to be predominant in most regions, e.g., 77% of the high-$PM_{2.5}$ days in JJ were attributed to the influence of LRT, US showed a greater occurrence of STL patterns accounting for 74% of occurrences, presumably attributable to its geographical location and characteristics of industrial emissions. Therefore, the JJ region, located westward of US, was more susceptible to the impact of LRT from outside sources of emissions.

As illustrated in Fig. 6, regions dominated by the STL mode were located mostly on the eastern side of South Korea, and these areas were often exposed to local circulation, leading to air stagnation in the region. Conversely, regions on the western side were characterized by the impacts of the LRT mode. Previous studies have predominantly focused on

Table 4
Matching of clusters in each region to clusters distinguished as LTP and STL.

Cluster/ Regions	SL	BS	DG	IC	GJ	DJ	US	SJ	GG	GW	CB	CN	JB	JN	GB	GN	JJ	Total
S_C1	SL_C4 (86)	BS_C3 (59)	DG_C3 (61)	IC_C2 (85)	–	–	US_C1 (90)	–	GG_C3 (94)	–	CB_C2 (97)	CN_C2 (69)	–	–	–	GN_C3 (63)	–	9
S_C2	SL_C2 (67)	–	DG_C1 (75)	–	–	–	–	–	–	GW_C1 (87)	–	–	–	–	GB_C3 (74)	–	JJ_C3 (31)	5
S_C3	–	BS_C2 (84)	–	–	GJ_C2 (78)	DJ_C1 (40)	US_C2 (97)	SJ_C1 (73)	GG_C4 (86)	–	CB_C3 (138)	CN_C3 (59)	JB_C2 (110)	JN_C3 (52)	GB_C1 (56)	GN_C2 (39)	–	12
S_C4	–	–	–	IC_C4 (37)	–	–	–	–	–	–	–	–	–	–	–	–	–	1
L_C1	SL_C3 (64)	BS_C1 (104)	DG_C2 (108)	IC_C1 (37)	GJ_C3 (75)	–	US_C3 (65)	SJ_C2 (67)	GG_C2 (74)	GW_C3 (104)	–	CN_C1 (70)	JB_C1 (162)	JN_C1 (49)	GB_C2 (123)	GN_C1 (50)	JJ_C2 (60)	15
L_C2	SL_C1 (91)	–	–	IC_C3 (58)	GJ_C1 (99)	DJ_C3 (65)	–	SJ_C3 (100)	GG_C1 (115)	GW_C2 (73)	CB_C1 (180)	CN_C4 (98)	JB_C3 (132)	–	–	–	JJ_C1 (45)	11
L_C3	–	–	–	IC_C5 (53)	–	DJ_C2 (38)	–	–	–	–	–	–	–	–	–	–	–	2
L_C4	–	–	–	–	–	DJ_C4 (36)	–	–	–	–	–	–	–	JN_C2 (36)	–	–	–	2
Total	4 (308)	3 (247)	3 (244)	5(270)	3 (252)	4 (179)	3 (252)	3 (240)	4 (369)	3 (264)	3 (415)	4 (296)	3 (404)	3 (137)	3 (253)	3 (152)	3 (136)	57

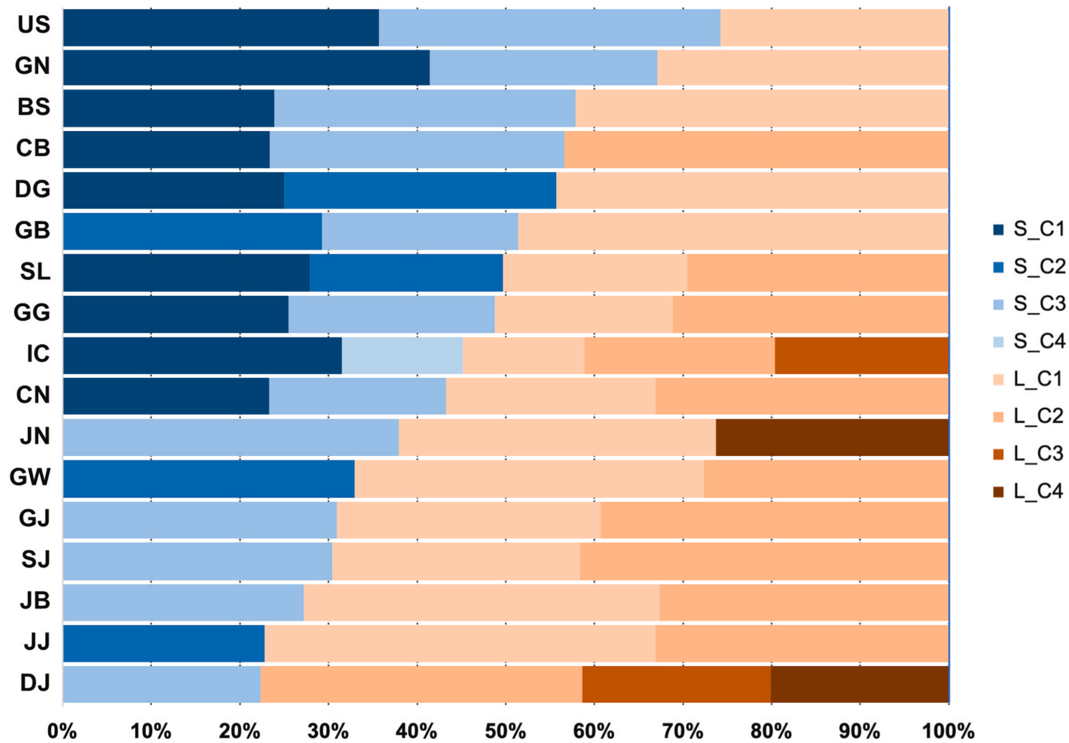

Fig. 5. Comparison of the contributions of wind patterns to high-$PM_{2.5}$ episodes in each region. STL contributions are shown in blue, and LRT contributions are shown in red. The 17 administrative regions are arranged in order of the STL contributions.

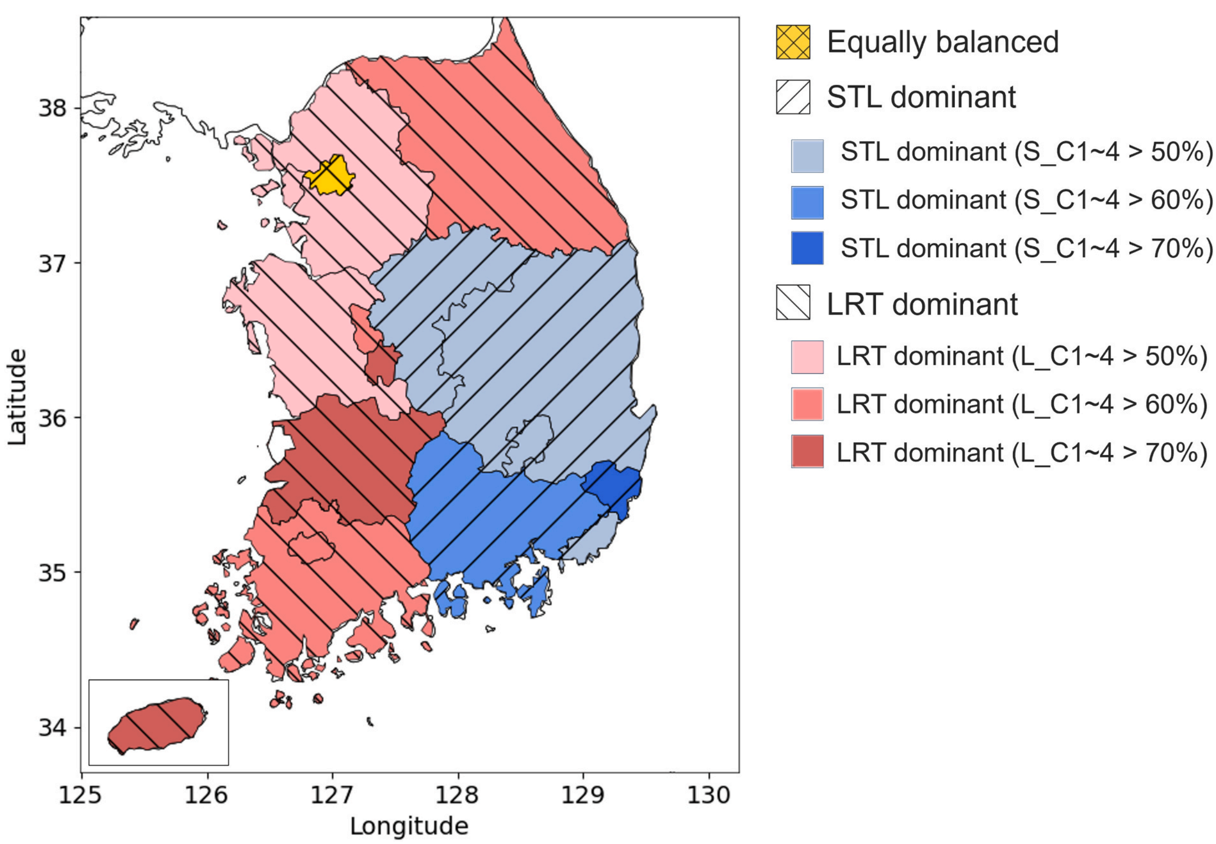

Fig. 6. Regional distributions of the predominance of wind patterns between LRT vs. STL in association with high-$PM_{2.5}$ in South Korea.

urban metropolitan areas, such as SMA (Choi et al., 2023; Park et al., 2005) and the Busan metropolitan area (Kim et al., 2021a). However, our study yielded region-to-region insights for air quality management on a national scale. Further detailed studies of regional-based local circulation and local emission characteristics are needed for some administrative regions, such as JB, JN, and GW.

4. Conclusion

We performed *k*-means cluster analysis to generate representative mesoscale wind field patterns associated with high-$PM_{2.5}$ episodes in all 17 administrative regions of South Korea during 2016–2020. These analyses corroborated the representative wind field patterns contributing to the high-$PM_{2.5}$ episodes for each region. We first identified the major wind patterns appearing during region-specific high-$PM_{2.5}$ episodes. We further extracted eight representative wind field patterns representing two major modes, i.e., LRT and STL modes.

Our results reveal that the overall LRT pattern in association with high $PM_{2.5}$ exhibited quite similar wind field patterns across the administrative regions, whereas region-specific distinctive patterns were also observed in some areas, which were mostly located along the southeastern or western coastal areas. Geographically, the LRT mode showed high frequencies in mostly western parts of the Korean Peninsula, whereas the STL mode was predominant near the southeastern regions. These observations suggest that geographical locations close to the upstream source regions in East China are susceptible to high $PM_{2.5}$ levels, and regional meteorological features also play a role. In addition, both the local nuances and the broader seasonal dynamics in each region should be considered for the effective mitigation of high-$PM_{2.5}$ episodes in each region. We anticipate that our observations regarding the mesoscale meteorological features of the 17 administrative regions in South Korea will be useful for the development of rational region-specific air pollution control measures.

Further comprehensive studies, including use of three-dimensional air quality models along with satellite image analysis, will provide a greater understanding of the impacts of wind patterns. Recent aircraft-based studies, such as SIAJQ and ASIA-AQ campaigns, are also good opportunities to precisely identify the pollutant source–receptor relations in South Korea to understand regional high-$PM_{2.5}$ episodes in both LTP and STL modes. We also anticipate that our results will be useful as a reference for interpretation of the relations between mesoscale meteorology and high-$PM_{2.5}$ episodes, as well as for the development of targeted $PM_{2.5}$ mitigation strategies in the administrative regions of South Korea.

CRediT authorship contribution statement

Daniel Choi: Conceptualization, Formal analysis, Writing – original draft, Data curation, Visualization. **Jeeyoung Ham:** Formal Analysis, Software, Investigation. **Gookyoung Heo:** Conceptualization, Data curation. **Soon-Hwan Lee:** Validation, Methodology. **Jung-Woo Yoo:** Software, Visualization. **Geum-Hee Yang:** Investigation, Validation. **Sohyun Jeon:** Formal analysis, Data curation. **Cheol-Hee Kim:** Conceptualization, Supervision, Formal analysis, Writing – review & editing, Methodology.

Declaration of competing interest

The authors declare that they have no known competing financial interests or personal relationships that could have appeared to influence the work reported in this paper.

Data availability

Data will be made available on request.

Acknowledgments

This study was supported by the Basic Science Research Program through the National Research Foundation of Korea (NRF) funded by the Ministry of Education (2020R1I1A2075417) and (2020R1A6A1A03044834). Special thanks are extended to the supercomputer management division at Korean Meteorological Administration (KMA) for granting us access to the DURU supercomputer resources and providing technical guidance and support.

Appendix A. Supplementary data

Supplementary data to this article can be found online at https://doi.org/10.1016/j.atmosenv.2024.120653.

References

Carro-Calvo, L., Ordonez, C., Garcia-Herrera, R., Schnell, J.L., 2017. Spatial clustering and meteorological drivers of summer zone in Europe. Atmos. Environ. 167, 496–510.

Chang, L.-S., Lee, G., Im, H., Kim, D., Park, S.-M., Choi, W.J., et al., 2021. Quantifying the impact of synoptic weather systems on high PM2.5 episodes in the Seoul Metropolitan Area, Korea. J. Geophys. Res. Atmos. 126.

Choi, D., Lee, H.-J., Chang, L.-S., Jo, H.-Y., Jo, Y.-J., Park, S.-Y., Yang, G.-H., Kim, C.-H., 2023. Distinct meteorological mode associated with high-PM2.5 episodes in Seoul, South Korea. J. Appl. Meteorol. Climatol. 62, 853–862.

Darby, L.S., 2005. Cluster analysis of surface winds in Houston, Texas, and the impact of wind patterns on ozone. J. Appl. Meteorol. 44, 1788–1806.

Ham, J., Suh, I., Lee, M., Kim, H., Kim, S., 2021. Elemental Carbon observed at a Peri-urban forest site near the Seoul metropolitan area as a Tracer of seasonal haze occurrence. Atmosphere 12, 1627.

Hwang, M.-K., Kim, Y.-K., Oh, I.-B., Lee, H.W., Kim, C.-H., 2007. Identification and interpretation of representative ozone distributions in association with the sea breeze from different synoptic winds over the coastal urban area in Korea. J. Air Waste Manag. Assoc. 57, 1480–1488.

Jeon, W., Lee, H.W., Lee, T., Yoo, J., Mun, J., Lee, S., Choi, Y., 2019. Impact of varying wind patterns on PM10 concentrations in the Seoul metropolitan area in South Korea from 2012 to 2016. J. Appl. Meteorol. Climatol. 58, 2743–2754.

Jin, L., Harley, R.A., Brown, N.J., 2011. Ozone pollution regimes modeled for a summer season in California's San Joaquin Valley: a cluster analysis. Atmos. Environ. 45, 4707–4718.

Jo, H.-Y., Kim, C.-H., 2013. Identification of long-range transported haze Phenomena and their meteorological features over northeast Asia. J. Appl. Meteorol. Climatol. 52, 1318–1328.

Kim, Y.-K., Song, S.-K., Lee, H.W., Kim, C.-H., Oh, I.-B., Moon, Y.-S., Shon, Z.-H., 2006. Characteristics of Asian dust transport based on synoptic meteorological analysis over Korea. J. Air Waste Manage. Assoc. 56, 306–316.

Kim, C.-H., Park, S.-Y., Kim, Y.-J., Chang, L.-S., Song, S.-K., Moon, Y.-S., Song, C.-K., 2012. A numerical study on indicators of long-range transport potential for anthropogenic particulate matters over northeast Asia. Atmos. Environ. 58, 35–44.

Kim, H.C., Kim, E., Bae, C., Cho, J.H., Kim, B.-U., Kim, S., 2017. Regional contributions to particulate matter concentration in the Seoul metropolitan area, South Korea: seasonal variation and sensitivity to meteorology and emissions inventory. Atmos. Chem. Phys. 17, 10315–10332.

Kim, J.H., Kim, H.J., Yoo, S.H., 2018a. Public value of Enforcing the PM2.5 concentration reduction policy in SouthSouth Korean urban areas. Sustainability 10, 1144.

Kim, C.H., Lee, H.J., Kang, J.E., Jo, H.Y., Park, S.Y., Jo, Y.J., Lee, J.J., Yang, G.H., Park, T., Lee, T., 2018b. Meteorological overview and signatures of long-range transport processes during the MAPS-Seoul 2015 campaign. Aerosol Air Qual. Res. 18 (9), 2173–2184. https://doi.org/10.4209/aaqr.2017.10.0398.

Kim, C.-H., Meng, F., Kajino, M., Lim, J., Tang, W., Lee, J.-J., Kiriyama, Y., Woo, J.-H., Sato, K., Kitada, T., Minoura, H., Kim, J., Lee, K.-B., Roh, S., Jo, H.-Y., Jo, Y.-J., 2021a. Comparative Numerical Study of PM2.5 in exit-and-entrance areas associated with transboundary transport over China, Japan, and Korea. Atmosphere 12, 469. https://doi.org/10.3390/atmos12040469.

Kim, J.-M., Lee, H.-J., Jo, H.-Y., Jo, Y.-J., Kim, C.-H., 2021b. Vertical characteristics of secondary aerosols observed in the Seoul and Busan metropolitan areas of Korea during KORUS-AQ and associations with meteorological conditions. Atmosphere 12, 1451.

Kim, C.-H., Jo, H.-Y., Jo, Y.-J., Lee, H.-J., Kim, J.-M., Lee, N.-M., Jeong, S.-Y., Baek, S.-H., Park, M.-J., Chang, L.-S., Song, C.K., 2023. Synoptic meteorological conditions and contributing factors to air quality during the SIJAQ campaign. Atmos. Environ. 309, 119939.

Lee, S., Ho, C.-H., Choi, Y.-S., 2011. High-PM10 concentration episodes in Seoul, Korea: Background sources and related meteorological conditions. Atmos. Environ. 45, 7240–7247.

Lee, H.-J., Kim, S.-W., Brioude, J., Cooper, O.R., Frost, G.J., Kim, C.-H., Park, R.J., Trainer, M., Woo, J.-H., 2014. Transport of NOx in East Asia identified by satellite and in situ measurements and Lagrangian particle dispersion model simulations. J. Geophys. Res. Atmos. 119, 2574–2596.

Lee, S., Ho, C.-H., Lee, Y.G., Choi, H.-J., Song, C.-K., 2013. Influence of transboundary air pollutants from China on the high PM10 episode in Seoul, Korea for the period October 16-20, 2008. Atmos. Environ. 77, 430–439.

Lee, H.-J., Jo, H.-Y., Kim, S.-W., Park, M.-S., Kim, C.-H., 2019a. Impacts of atmospheric vertical structures on transboundary aerosol transport from China to South Korea. Sci. Rep. 9, 13040.

Lee, H.-J., Jo, H.-Y., Park, S.-Y., Jo, Y.-J., Jeon, W., Ahn, J.-Y., Kim, C.-H., 2019b. A case study of the transport/transformation of air pollutants over the Yellow Sea during the MAPS 2015 campaign. J. Geophys. Res. Atmos. 124, 6532–6553.

Leung, D.M., Tai, A.P.K., Mickley, L.J., Moch, J.M., van Donkelaar, A., Shen, L., Martin, 2018. Synoptic meteorological modes of variability for fine particulate matter (PM2.5) air quality in major metropolitan regions of China. Atmos. Chem. Phys. 18, 6733–6748.

NIER (National Institute of Environmental Research), 2018. 2015 national air pollutants emission. https://www.air.go.kr/article/view.do?boardId=7&articleId=132&boardId=7&menuId=48&currentPageNo=1.

Oh, H.-R., Ho, C.-H., Kim, J., Chen, D., Lee, S., Choi, Y.-S., et al., 2015. Long-range transport of air pollutants originating in China: A possible major cause of multi-day high-PM10 episodes during cold season in Seoul, Korea. Atmos. Environ. 109, 23–30.

Oh, H.R., Ho, C.H., Koo, Y.S., Baek, K.G., Yun, H.Y., Hur, S.K., et al., 2020. Impact of Chinese air pollutants on a record-breaking PMs episode in the Republic of Korea for 11–15 January 2019. Atmos. Environ. 223, 117262.

Oh, I.-B., Kim, Y.-K., Lee, H.W., Kim, C.-H., 2006. An observational and numerical study of the effects of the late sea breeze on ozone distributions in the Busan metropolitan area, Korea. Atmos. Environ. 40, 1284–1298.

Oh, S.-S., Lee, H.-J., Kim, M.-S., Park, M.-S., Kim, C.-H., 2024. Aerosol-heat flux interactions in the boundary layer during the SIJAQ campaign. Atmos. Environ. 319, 120306.

Park, I.-S., Choi, W.-J., Lee, T.-Y., Lee, S.-J., Han, J.-S., Kim, C.-H., 2005. Simulation of long-range transport of air pollutants over Northeast Asia using a comprehensive acid deposition model. Atmos. Environ. 39, 4075–4085.

Park, K., Yoon, T., Shim, C., Kang, E., Hong, Y., Lee, Y., 2020. Beyond Strict Regulations to Achieve Environmental and Economic health—an optimal $PM_{2.5}$ mitigation policy for Korea. Int. J. Environ. Res. Publ. Health 17, 5725.

Park, D.-H., Kim, S.-W., Kim, M.-H., Yeo, H., Park, S.S., Nishizawa, T., Shimizu, A., Kim, C.-H., 2021. Impacts of local versus long-range transported aerosols on PM_{10} concentrations in Seoul, Korea: an estimate based on 11-year PM10 and lidar observations. Sci. Total Environ. 750, 141739.

Seo, J., Kim, J.Y., Youn, D., Lee, J.Y., Kim, H., Lim, Y.B., Kim, Y., Jin, H.C., 2017. On the multiday haze in the Asian continental outflow: the important role of synoptic conditions combined with regional and local sources. Atmos. Chem. Phys. 17, 9311–9332.

Seo, J., Park, Kim, J.Y., Youn, D., Lim, Y.B., Kim, Y., 2018. Effects of meteorology and emissions on urban air quality: A quantitative statistical approach to long-term records (1999-2016) in Seoul, South Korea. Atmos. Chem. Phys. 18 (21), 16121–16137.

Souri, A.H., Choi, Y., Li, X., Kotsakis, A., Jiang, X., 2016. A 15-year climatology of wind pattern impacts on surface ozone in Houston, Texas. Atmos. Res. 174–175, 124–134.

Tai, A.P.K., Mickley, L.J., Jacob, D.J., Leibensperger, E.M., Zhang, L., Fisher, J.A., Pye, H.O.T., 2012. Meteorological modes of variability for fine particulate matter ($PM_{2.5}$) air quality in the United States: Implications for $PM_{2.5}$ sensitivity to climate change. Atmos. Chem. Phys. 12, 3131–3145.

Wang, Z., Pan, X., Uno, I., Chen, X., Yamamoto, S., Zheng, H., et al., 2018. Importance of mineral dust and anthropogenic pollutants mixing during a long-lasting high PM event over East Asia. Environ. Pollut. 234, 368–378.

Yang, G.-H., Jo, Y.-J., Lee, H.-J., Song, C.-K., Kim, C.-H., 2020. Numerical sensitivity Tests of volatile organic compounds emission to PM2.5 formation during heat Wave period in 2018 in two southeast Korean cities. Atmosphere 11, 331.

Zhao, S., Feng, T., Tie, X., Long, X., Li, G., Cao, J., et al., 2018. Impact of climate change on Siberian High and wintertime air pollution in China in past two decades. Earth's Future 6 (2), 118–133.